Supporting Information

Insights on the origin of catalysis on glycine N-methyltransferase from computational modelling

Katarzyna Świderek,[1,2] Iñaki Tuñón,[3,*] Ian H. Williams,[2] Vicent Moliner.[1,2,*]

1. Departament de Química Física i Analítica; Universitat Jaume I, 12071 Castellón (Spain)
2. Department of Chemistry, University of Bath, Bath BA2 7AY (United Kingdom)
3. Departament de Química Física, Universitat de València, 46100 Burjasot, (Spain)

Table of Contents

1. Molecular dynamic simulations

Table S1. SAM substrate missing (a) charges (in a.u.) and (b) impropers determined using antechamber module available in AmberTools.[1,2]

a) CHARGES

Atom	Element	Atom Type	Mulliken Charge
1	N	n4	-0.049
2	C	c3	-0.196
3	C	c	0.349
4	O	o	-0.367
5	O	o	-0.523
6	C	c3	-0.138
7	C	c3	-0.567
8	S	s4	1.541
9	C	c3	-0.703
10	C	c3	-0.650
11	C	c3	0.020
12	O	os	-0.318
13	C	c3	-0.016
14	O	oh	-0.297
15	C	c3	-0.027
16	O	oh	-0.313
17	C	c3	0.166
18	N	na	-0.216
19	C	cc	-0.051
20	N	nd	-0.087
21	C	ca	-0.245
22	C	ca	0.257
23	N	nh	-0.327
24	N	nb	-0.252
25	C	ca	0.016
26	N	nb	-0.285
27	C	ca	0.078
28	H	hn	0.281
29	H	hn	0.241
30	H	hx	0.197
31	H	hc	0.112
32	H	hc	0.117
33	H	h1	0.157
34	H	h1	0.154
35	H	h1	0.160
36	H	h1	0.149
37	H	h1	0.142
38	H	h1	0.133
39	H	h1	0.158
40	H	h1	0.138

41	H	h1	0.143
42	H	ho	0.224
43	H	h1	0.117
44	H	ho	0.237
45	H	h2	0.175
46	H	h5	0.211
47	H	hn	0.261
48	H	hn	0.255
49	H	h5	0.175
50	H	hn	0.263
Total Mulliken Charge =			**1.000**

b) IMPROPERS

c3-o -c -o	1.1	180.0	2.0	General improper torsional angle (1 general atom type)
c3-ca-na-cc	1.1	180.0	2.0	Using default value
h5-na-cc-nd	1.1	180.0	2.0	Using default value
ca-ca-ca-nd	1.1	180.0	2.0	Using default value
ca-nb-ca-nh	1.1	180.0	2.0	Using default value
ca-hn-nh-hn	1.1	180.0	2.0	Using default value
h5-nb-ca-nb	1.1	180.0	2.0	Using default value
ca-na-ca-nb	1.1	180.0	2.0	Using default value

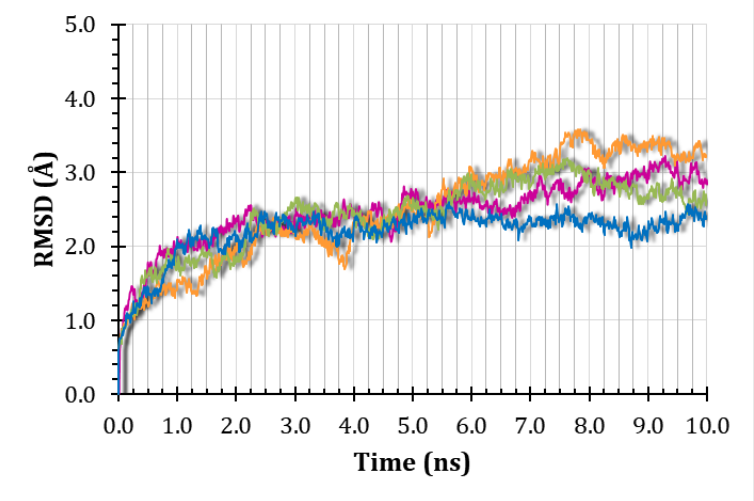

Figure S1. Time dependence of root mean square deviation (**RMSD**) from four independent 10 ns MD-NVT simulations for Wild Type (magenta), Y21F (blue), Y21A (green) and Y21G (orange) variant of GNMT enzyme at 293K.

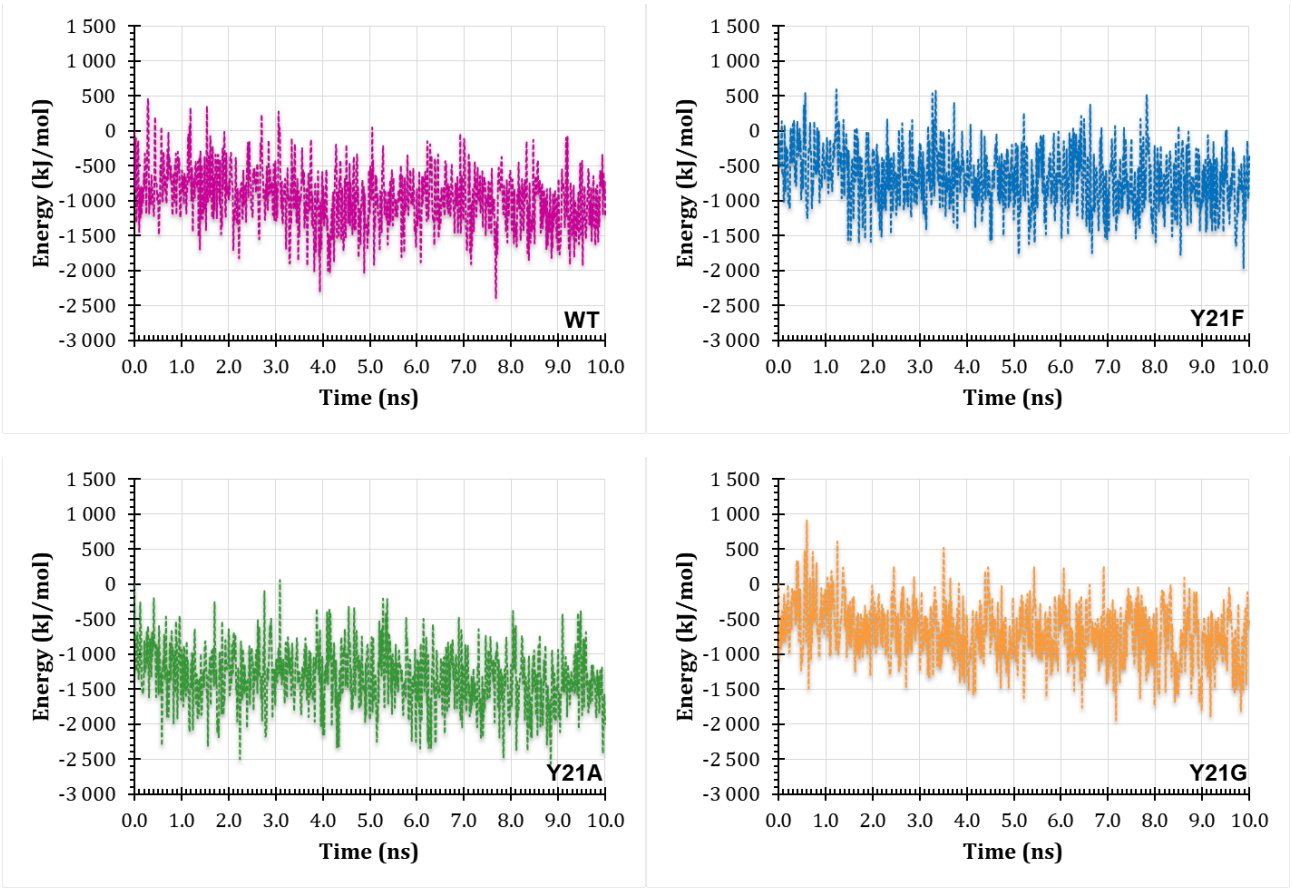

Figure S2. Time dependence of total energy from four independent 10ns MD-NVT simulations for Wild Type (magenta), Y21F (blue), Y21A (green) and Y21G (orange) variant of GNMT enzyme at 293K.

Table S2. Average values of DAD (donor-acceptor distance) and MAD (methyl-acceptor distance) obtained from 10 ns of NPT MD simulations of the ternary reactant complex at two different pressures: 1 and 1000 bar) and from 10 ns of NVT MD simulations. All simulations run at 293 K. AMBER force field was used as implemented in NAMD package (see ref 43 of the text). The constant pressure simulations were carried out using the Langevin piston method.

		DAD (Å)	MAD (Å)
NPT	P (bar)		
	1	5.0 ± 0.7	3.4 ± 0.8
	1000	5.0 ± 0.4	3.4 ± 0.5
NVT		4.8 ± 0.1	3.4 ± 1.1

2. Free energy calculations

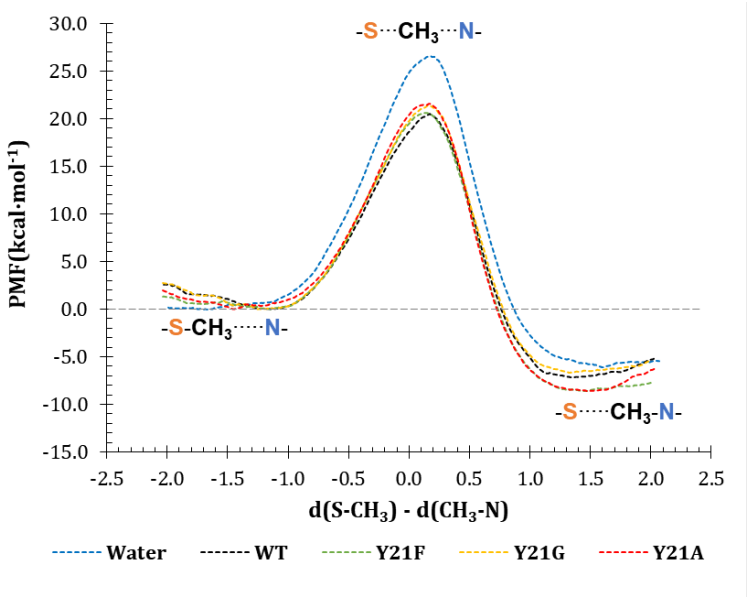

Figure S3. AM1/MM PMFs (at 293K) for the Methylation of Glycine (Scheme 2) in aqueous solution (blue line) and catalyzed by wild type (black line), Y21F (green line), Y21G (yellow line) and Y21A (red line) variants of GNMT. Distances are in Å and energies in kcal·mol^{-1}.

3. Structural Analysis

Table S3. Average DAD (in Å) and S-C-N angle (in degrees) obtained in the reactant state (RS) and transition state (TS) for the methylation of glycine in aqueous solution and in the different forms of the recombinant rat-liver GNMT obtained at AM1/MM level.

	DAD		S-C-N	
	RS	TS	RS	TS
Water	4.79 ± 0.19	4.24 ± 0.10	129.0 ± 11.0	172.4 ± 4.6
WT	4.76 ± 0.09	4.10 ± 0.10	162.4 ± 6.8	171.5 ± 4.0
Y21F	4.71 ± 0.10	4.23 ± 0.10	163.1 ± 7.3	172.5 ± 3.5
Y21A	5.01 ± 0.08	4.11 ± 0.11	168.3 ± 5.7	170.1 ± 3.9
Y21G	4.82 ± 0.09	4.15 ± 0.11	164.8 ± 6.5	169.6 ± 4.4

Figure S4. Schematic representation of the interactions established with the hydrogen atoms of the transferring methyl group of SAM in water and in the binary GNMT-SAM complex optimized at M06-2X/MM level.

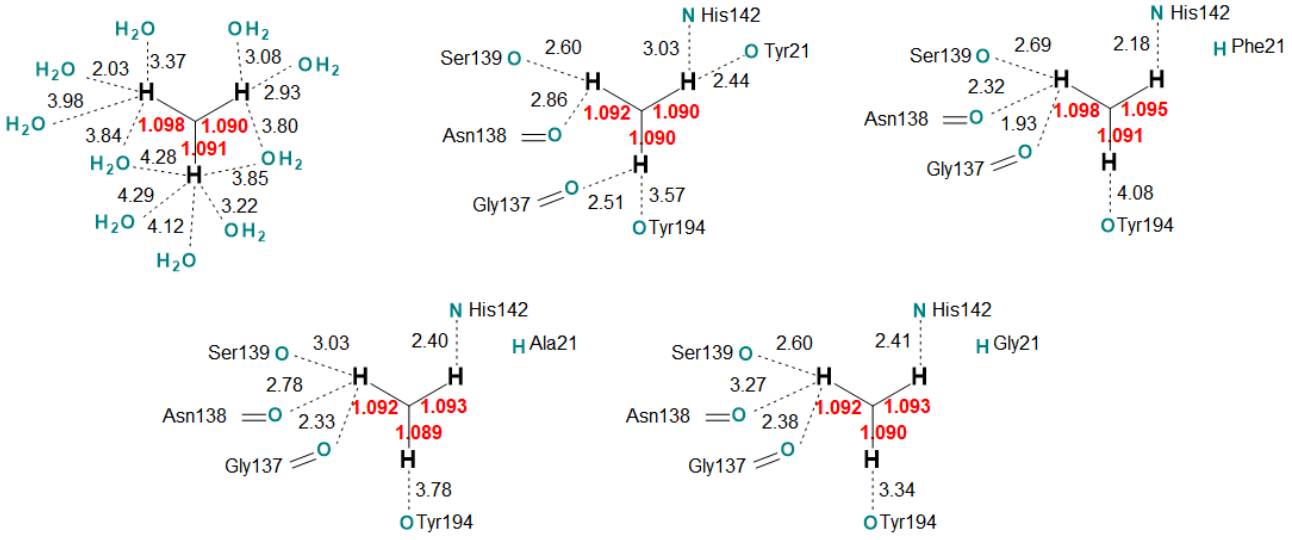

Figure S5. Depiction of the catalytic residues at the active site from structures of the GNMT:SAM binary complex optimized at M06-2X/MM level in A) WT GNMT; B) Y21F GNMT; C) Y21A GNMT; and D) Y21G GNMT Distances are in Å and the angle in degrees.

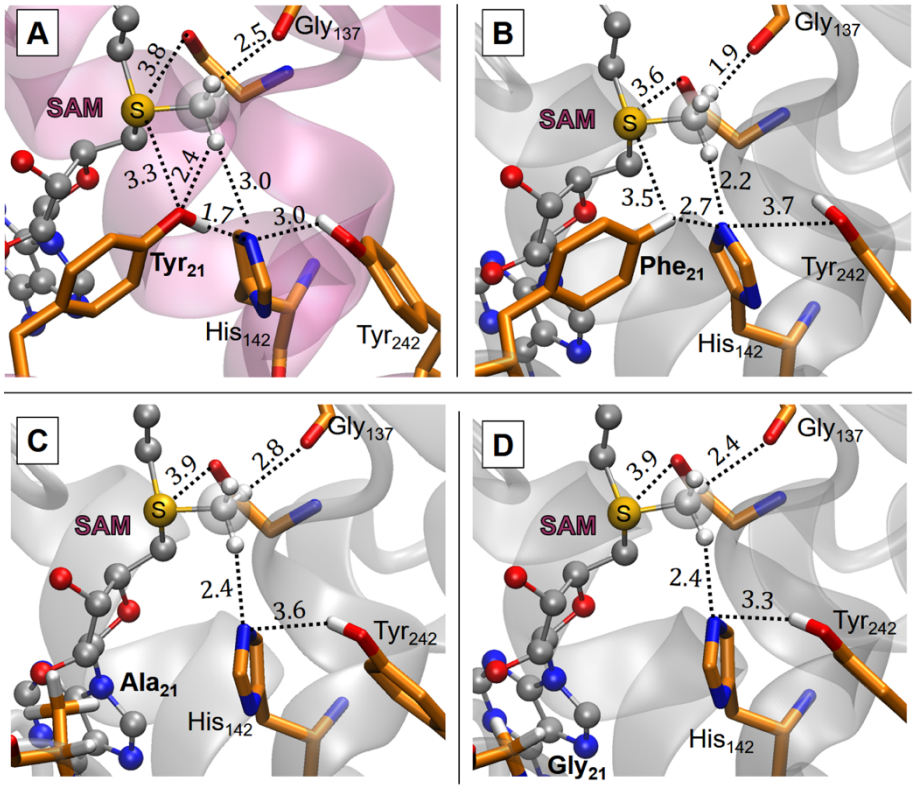

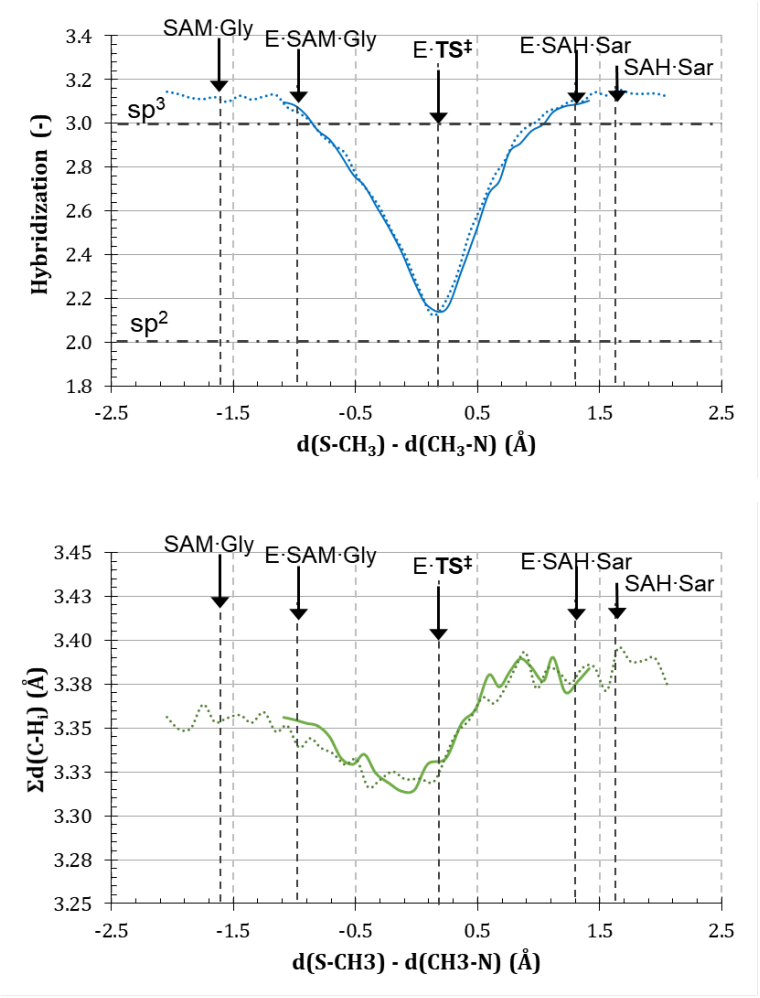

Figure S6. Change in C-hybridization along reaction coordinate. Dot line in water solid line for WT (upper plot) and in the sum of three C-H bonds in transferred methyl group along reaction coordinate. Dot line in water solid line for WT (bottom plot).

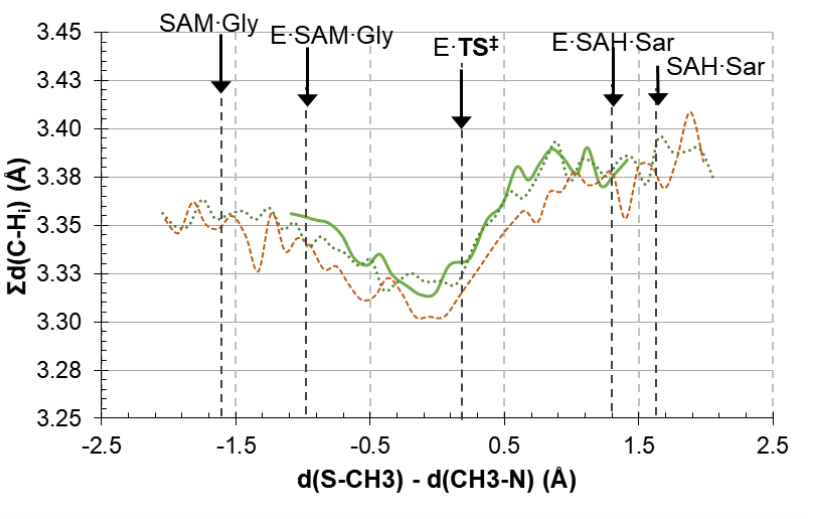

Figure S7. Sum of C-H bond distances of the transferring methyl group along the reaction coordinate gas phase (orange dashed line), in water (green dotted line) and in the WT GNMT (green solid line). Results obtained at AM1/MM level. Positions of the different states located in the enzyme catalyzed reaction are indicated as dashed vertical lines.

4. Kinetic and Binding Isotope Effects

Table S4. 1º $^{12}C/^{14}C$ and 2º $^{1}H_3/^{3}H_3$ KIEs computed from the GNMT:SAM binary complex at M06-2X/6-31G+(d,p)/MM level at 293 K. Values computed from 3x3 structures combinations of RS and TS.

	2º $^{1}H_3/^{3}H_3$ KIE[b]	1º $^{12}C/^{14}C$ KIE[b]
water	0.680 ± 0.055	1.110 ± 0.011
WT	0.630 ± 0.016	1.116 ± 0.003
Y21F	0.659 ± 0.023	1.121 ± 0.004
Y21A	0.656 ± 0.035	1.120 ± 0.007
Y21G	0.638 ± 0.031	1.117 ± 0.005

Table S5. 1º $^{12}C/^{14}C$ and 2º $^{1}H_3/^{3}H_3$ KIE, computed from the GNMT:SAM:Gly ternary complex at AM1/MM level at 293 K. Values computed from 10x10 structures combinations of RS and TS, respectively.

AM1/MM		
	2º KIE ($^{1}H_3/^{3}H_3$)	1º KIE ($^{12}C/^{14}C$)
water	0.762 ± 0.023	1.114 ± 0.005
WT	0.809 ± 0.023	1.104 ± 0.003
Y21F	0.761 ± 0.019	1.109 ± 0.003
Y21A	0.795 ± 0.016	1.103 ± 0.007
Y21G	0.751 ± 0.018	1.101 ± 0.004

Table S6. BIEs for the binding of SAM to the active site of the proteins, computed at M06-2X/6-31G+(d,p)/MM level at 293 K. Values computed from 3 x 3 structures combinations of SAM in water and in the active site of the different GNMT variants.

	$^{1}H_3/^{3}H_3$ BIE	$^{12}C/^{14}C$ BIE
WT	1.162 ± 0.017	0.998 ± 0.003
Y21F	1.049 ± 0.034	0.992 ± 0.004
Y21A	1.058 ± 0.053	0.995 ± 0.003
Y21G	1.085 ± 0.049	0.990 ± 0.006